Detection of Capillary Vessels in Optical Coherence Tomography Based on a Probabilistic Kernel

Eva Dittrich[a,b]*, Radhouène Neji[c,d], Tilman Schmoll[e], Sabine Schriefl[f], Christian Ahlers[f], Rainer A. Leitgeb[e], Georg Langs[a]

[a]Computational Image Analysis and Radiology Lab, Department of Radiology, Medical University of Vienna, Vienna, Austria
[b]Pattern Recognition & Image Processing Group, Institute of Computer Aided Automation, Vienna University of Technology, Vienna, Austria
[c]GALEN Group, Laboratoire des Mathématiques Appliquées aux Systèmes, Ecole Centrale Paris, Châtenay-Malabry, France
[d]Département Signaux et Systèmes Electroniques, Ecole Supérieure d'Electricité, Gif-sur-Yvette, France
[e]Center for Biomedical Engineering and Physics, Christian Doppler Laboratory, Medical University of Vienna, Vienna, Austria
[f]Department of Ophthalmology, Advanced Imaging Group, Medical University of Vienna, Vienna, Austria

Abstract. Optical coherence tomography is a non-invasive method used for the three dimensional in-vivo observation of the human eye's retinal layers. In this paper we propose an approach that segments the fine capillary vessels of the retina in this data. The whole processing is computed in 3D. The method is based on vessel filtering and a subsequent detection of the individual vessel points by means of a probabilistic kernel. By embedding the points in a diffusion map based on their structural and spatial properties, we are able to use the joint behavior of the individual vessel segments, to boost the detection and delineation performance in the highly noisy data. We investigate the benefit of the probabilistic kernel embedding and report experimental results on real data sets. They demonstrate the additional benefit of the embedding to accurately segment the vessels.

1 Introduction

Detecting vascular networks is an important issue in medical image analysis. It allows to discover pathologies, that can have serious consequences; it is important during the planning of interventions, and can serve as a precursor to the study of the function of certain anatomical structures. *Optical Coherence Tomography (OCT)* is a modality that can capture the retina layers of the eye (see Fig. 1). The analysis of the capillary network in the retina is crucial for the study and diagnosis of diseases, that result in a change of the vascular patterns, and the blood flow. Examples are diabetic retinopathy, age-related macular degeneration (AMD) or glaucoma (which are the three leading causes of blindness in the USA [1]). OCT allows for an observation of these very fine networks, but the capillary vessels located in the ganglion cell layer of the retina are difficult to identify because of the high amount of noise.

In this paper we present an approach to detect capillary vessels in OCT data based on probabilistic kernels reflecting the mutual relations of vessel points, and a spectral embedding [2] of the local structure description. Due to the high amount of noise in the OCT data it is necessary to integrate the information of larger vessel segments in the detection process. We do this by embedding the initial vessel candidate positions in a diffusion map that captures local structure and mutual spatial relations of the vessel points. The positions in this map can be used to efficiently distinguish between vessels and background noise.

State of the Art Initial vessel detection filters were proposed in 1998 by [3] and [4]. In both cases a vesselness value is computed for each point of the volume (or image) by using the eigenvalues and eigenvectors of the Hessian matrix. Vessel enhancing filters like those proposed in [5] and [6] are also based on the eigenvalue decomposition of the Hessian matrix. Another promising approach for centerline detection was proposed in [7], and a good overview of vessel extraction methods is given in [8]. A similar goal to the work presented in this paper is aimed at the segmentation of vessels in Doppler Optical Coherence Angiography retinal images by [9]. The authors demonstrate a retinal blood flow quantification with a retinal vessel segmention on 2D retinal vessel images and 2D cross-sectional flow images. However, they are segmenting vessels with far larger diameter and contrast. To the best of our knowledge, no work

*eva.dittrich@student.tuwien.ac.at. This research has been supported by the Austrian National Bank OeNB (12537, COBAQUO).

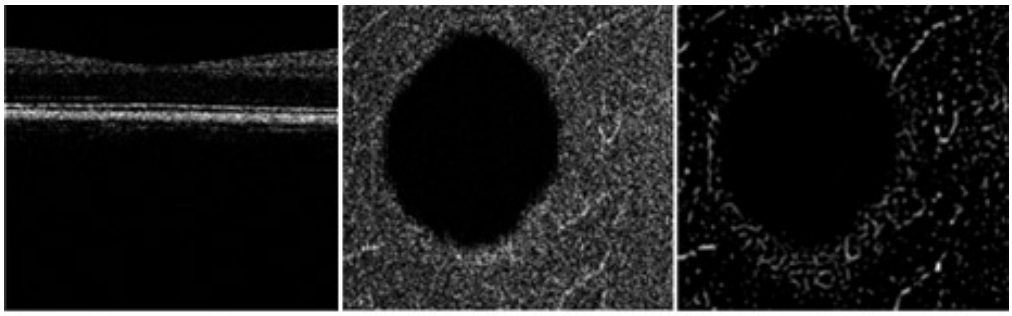

(a) (b) (c)

Figure 1. OCT data of the human retina. (a) B-scan (a set of A-scans which are the vertical lines in the image), and (b) en-face/top view. We are detecting capillaries in the layers surrounding this one. Note the high amount of noise. (c) The same layer after standard vessel filtering: vessels are enhanced, but there is still substantial clutter left. This is dealt with by the embedding approach described in this paper.

exists that tackles the segmentation of the fine capillary vessels in the ganglion cell layer of the human retina which are about 10 μm in diameter. The challenge is to find the capillary vessels even though the background noise is high and separates individual vessel segments. Interesting related work is dealing with the segmentation of muscles and muscle fibres in diffusion tensor data [10].

2 Method outline

Our method is divided into three steps: 1. candidate points for vessels are detected in the volume [6]. 2. A description of the corresponding local structure, that reflects the vessel is acquired from the OCT data. 2. These candidate points are embedded into a map based on their mutual spatial configuration and local structure, and the vessels are detected based on the positions in this map. This last part is described in Sec. 5 and its use in the detection of capillary vessels is the main contribution of the paper.

3 Detecting vessel candidate points

As a first step, we are detecting candidates for vessels in the OCT data based on a standard filtering introduced in [6]. It enhances tubular structures based on the eigenvalues of the Hessian matrix at each position. Assuming that the largest eigenvalue λ_1 (with $\lambda_1 > \lambda_2 > \lambda_3$) is close to 0 for tubular structures, and the remaining two $\lambda_2, \lambda_3 < 0$, one can estimate the vesselness based on λ_1, and λ_2. To account for signal strength fluctuations along the vessel axis, in [6] the two cases $\lambda_1 > 0$ (vessel is interrupted), and $\lambda_1 \leq 0$ (vessel or blob) are treated differently. Thus the result is dependent on 3 parameters: σ represents the approximate diameter of the vessel to be looked for, α_1 quantifies the influence of noise removal in the case of $\lambda_1 \leq 0$, and α_2 affects the reconstruction of disconnected parts in the case of $\lambda_1 > 0$, (in general: $\alpha_1 < \alpha_2$). In Fig. 1(c) the result of the vessel enhancement is illustrated for the retina OCT data. A part of the noise is suppressed by this step, but the local nature of the filtering is not able to differentiate between components of the retina background structure and the capillaries. We treat the result as vessel candidates, and in the following two sections we describe how to verify them based on a kernel, that takes both the local structure, and the mutual spatial relations of the candidates into account.

4 Describing the local vessel structure

Each point resulting from the previous step is considered as a candidate point. To describe the local structure the structure tensor $\mathcal{S}$ (see Eq. 1; I_x is the first partial derivative $\frac{\delta I}{\delta x}$, etc.) is computed for each candidate point to describe the local intensity variation. Note that this tensor is guaranteed to be positive definite.

$$\mathcal{S} = \begin{pmatrix} I_x^2 & I_x I_y & I_x I_z \\ I_y I_x & I_y^2 & I_y I_z \\ I_z I_x & I_z I_y & I_z^2 \end{pmatrix} \tag{1}$$

In tubular structures like the vessel, an eigenvalue decomposition of this tensor results in two eigenvectors perpendicular to the tube direction associated with large eigenvalues. The third smallest eigenvalue is associated with the direction of the vessel, and the corresponding small intensity derivative. Based on this structure we now create a local description that can be interpreted as a probability distribution reflecting the typical neighborhood relations of vessel points. For

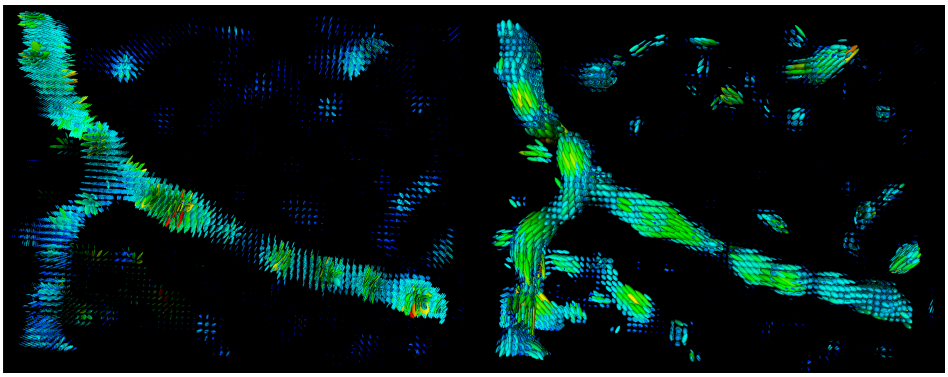

Figure 2. Visualizations of the structure tensors and the modified tensors by ellipsoids defined by eigenvectors and eigenvalues for a section of the retina. Left: the structure tensors indicate the gradient directions orthogonal to the vessel direction; right: the modified tensors result in ellipsoids that follow the vessel direction, and are used for the mapping of the vessel points.

each point the distribution indicates the probability to find a neighboring vessel point at a certain position.

On the basis of the structure tensor with eigenvalues λ_i, $i = \{1, 2, 3\}$ we generate a modified tensor that reflects this distribution by the altering the eigenvalues λ_i^*, $i = \{1, 2, 3\}$ (see Eq. 2, with $\epsilon < 1$ and $\gamma << 1$) which define a modified tensor similar to a segmentation term in [11]. A normalization is also conducted to suppress isotropic structure tensors (see Eq. 3). In Fig. 2 we illustrate the difference between the structure tensor and the modified structure tensor for a synthetic data set with a strong tubular structure, and a section of the retina containing a capillary vessel.

$$\lambda_i' = e^{(-\gamma|\lambda_{i_{old}}|)} + \epsilon \quad \text{for } i = \{1, 2, 3\} \tag{2}$$

$$\lambda_1 \leq \lambda_2 \leq \lambda_3, \quad \lambda_i^* = \frac{\lambda_i'}{\lambda_1 \lambda_2} \quad \text{for } i = \{1, 2, 3\} \tag{3}$$

For each candidate point we now have the position and a tensor that describes the local data structure. This is the basis for the embedding of the vessel points in a map that reflects the probabilities of the vessel candidates to be neighbors in a vessel structure.

5 Finding Vessels in a Mapping based on Probabilistic Kernels

To establish the mapping, we first need a distance between the vessel candidates. We use a distance measure proposed in [10]. It was originally created to cluster diffusion tensors and fiber tracts in the human skeletal muscles. It uses a kernel that encompasses spatial localization as well as tensor orientation in such a way that a feature space is computed, in which those tensors pointing into the same direction and corresponding to locations along this very same direction, will be closer than those not lying on the same fiber tract. Let us consider two tensors T_1 and T_2 localized at x_1 and x_2 respectively, and a diffusion time t that determines the size of the kernel - it can be interpreted as the time a particle in a diffusion process is given to reach a certain location. t acts as a scale parameter, and larger values emphasize the role of the kernel compared to the role of mutual location. We suppose that $t\,T_1$ and $t\,T_2$ encode the covariance information of Gaussian diffusion probabilities $p_1(y|x_1, t, T_1)$ and $p_2(y|x_2, t, T_2)$ at locations x_1 and x_2 respectively, with y being the displacement of the tensor. Following [10], this leads us to consider the expected likelihood kernel k_t between the pairs (T_1, x_1) and (T_2, x_2), which is defined as the expectation of Gaussian probability $p_2(y|x_2, t, T_2)$ given the probability of $p_1(y|x_1, t, T_1)$ and has a closed-form expression (see Eq. 4; for more details the authors refer to [10]).

$$k_t((T_1, x_1), (T_2, x_2)) = \int p_1(y|x_1, t, T_1) p_2(y|x_1, t, T_1) dy \tag{4}$$

$$= \frac{1}{\sqrt{\det(T_1 + T_2)}} \exp\left(-\frac{1}{4t}(x_1 - x_2)^t (T_1 + T_2)^{-1}(x_1 - x_2)\right) \tag{5}$$

A subsequent mapping into a feature space with chosen dimension according to the kernel Gram matrix enables a differentiation of the tensors in order to separate tubular structures from background noise. In this feature space, the points are arranged according to the previously computed distance measure. The points belonging to background regions collapse into an area closest to the origin compared to the other points. This is due to the fact that leading

eigenvectors of the Gram matrix are expected to represent the relevant information in the data while the eigenvectors corresponding to the smaller eigenvalues correspond to noisy structures. Therefore background noise is expected to have a projection close to the origin in the feature space since it lies in the subspace generated by eigenvectors corresponding to small eigenvalues. Thus, by classifying points in the diffusion map with

$$||x - x_0|| < \epsilon \tag{6}$$

as background (with ϵ determining the distance from the origin), it is possible to differentiate tensors describing tubular structures from those of background noise: all points in the feature space within a sufficiently short distance to the origin are eliminated.

6 Results

Setup For our experiments 3 segments of OCT volumes of the human retina, with a size of $15 \times 50 \times 70$, $25 \times 70 \times 50$ and $25 \times 60 \times 70$ were used. For each of the volumes the same procedure was conducted: First, the vessel enhancing filter was applied (we used the implementation available in MATITK). The according parameters were set as follows: σ = 2 , α_1 = 0.9, and α_2 = 1. For the computation of the structure tensor, the parameters were chosen as $\epsilon = 0.1$ and $\gamma = 0.025$. The distance matrix was only computed for points that lie within a local range of ± 5 voxel and whose first eigenvalue $\lambda_1 \geq 5$. After the mapping into the feature space the points having a distance of $||x - x_0|| < \epsilon$ (for $\epsilon = 2 * 10^{-15}$) were eliminated. Parameters were the same for all examples.

Results For the validation a standard of reference annotation of the vessels in the volumes was performed by a medical expert. The error is reported as the wrongly detected vessel points (false positives) and those wrongly classified as background (false negatives). To evaluate the behaviour of our method, the results of the vessel detector were compared to our final results after the embedding and the false positives and false negatives were calculated for each of them. See Tab. 1 for the error rates of each OCT volume. The final results for each dataset are depicted in Fig. 3. The false positives are reduced significantly, while the number of false negatives increases slightly which is mainly due to the fact that there is no sharp border between vessel points and background points, leading to a part of annotated vessel points being omitted. The accurate separation and increase of the sensitivity is subject of ongoing work.

Volume	vessel detector based on [6]		proposed method	
	FP	FN	FP	FN
OCT 1	2031	2066	1204	2127
OCT 2	6507	3017	1233	3029
OCT 3	12275	847	1367	862

Table 1. False positives and false negatives for the plain vessel detector and the proposed method.

7 Conclusion and Outlook

We propose a method to automatically detect capillary vessel structures in OCT data. The approach is based on an embedding of the vessel points in a feature space based on their mutual spatial and structure relations. The vessels have a diameter of about $10\mu m$ and are hard to be distinguished from the background by standard methods. Due to the high background noise and the small diameter, standard methods to segment the vessels fail. The embedding is able to integrate vessel information over sets of candidates, and thus exploits the natural structure of the capillary vessels - elongated tubes - to deal with noisy data, where parts of the vessels are missing or lost in clutter. Future work will focus on the improvement of the sensitivity of the method, and the further study of the embedding.

References

1. M. Sofka & C. Stewart. "Retinal vessel centerline extraction using multiscale matched filters, confidence and edge measures." *Medical Imaging* Jan 2006.
2. R. Coifman & S. Lafon. "Diffusion maps." *Applied and Computational Harmonic Analysis* Jan 2006.
3. A. Frangi, W. Niessen, K. Vincken et al. "Multiscale vessel enhancement filtering." *LECTURE NOTES IN COMPUTER SCIENCE* 1998.
4. K. Krissian, G. Malandain, N. Ayache et al. "Model based multiscale detection of 3d vessels." *Biomedical Image Analysis* 1998.
5. R. Manniesing, M. Viergever & W. Niessen. "Vessel enhancing diffusion: A scale space representation of vessel structures." *Medical Image Analysis* **10(6)**, pp. 815–825, Dec 2006.

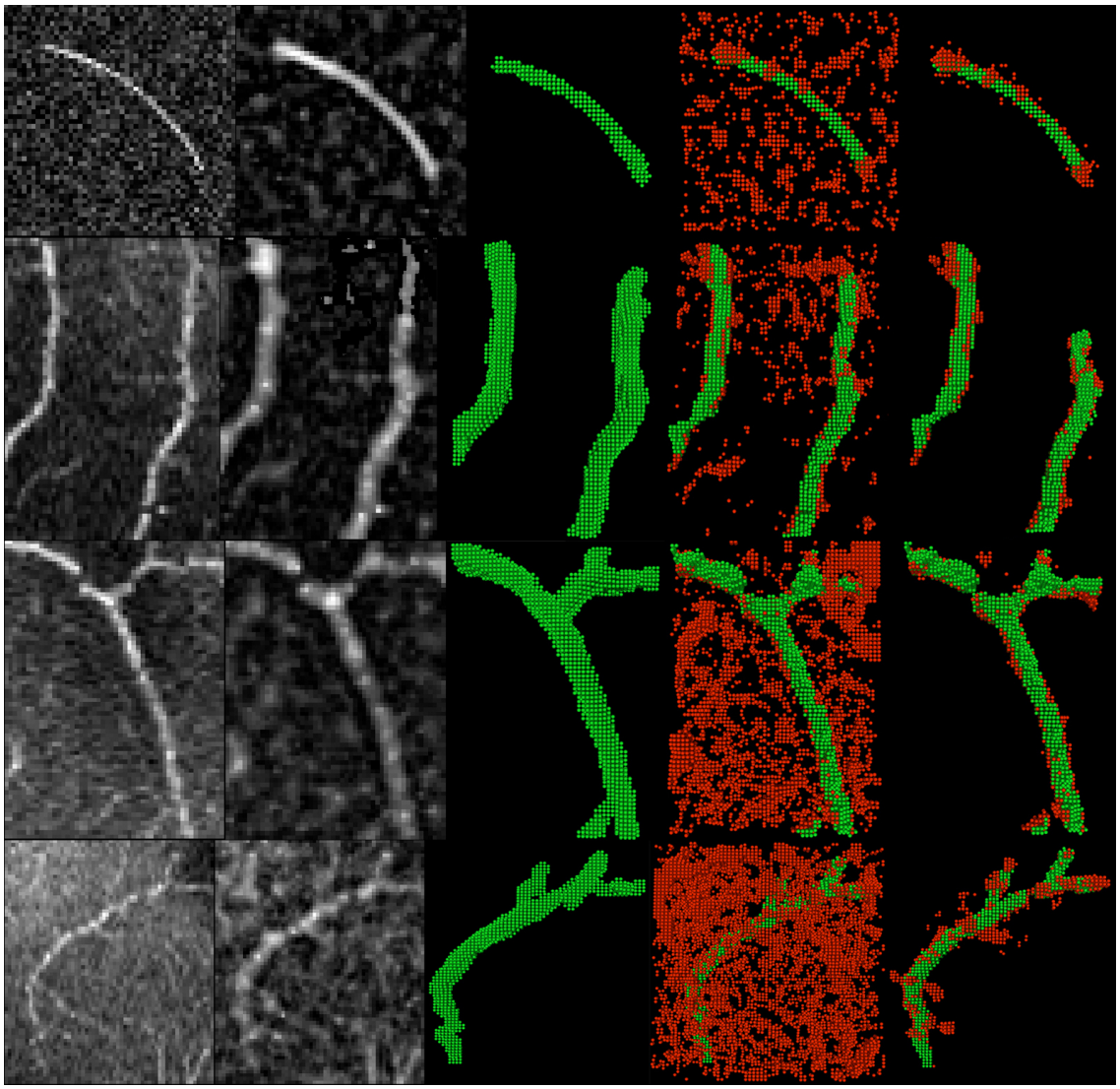

Figure 3. Results for one synthetic (top row) and three sections of OCT volumes. 1st column: original volume. 2nd column: filtered volume. 3rd column: groundtruth data. 4th column: result from vessel detector [6]. 5th column: result of our method. Note the reduced background noise. Red points represent FP, green points are TP.

6. Y. Sato, S. Nakajima, N. Shiraga et al. "3d multi-scale line filter for segmentation and visualization of curvilinear structures in medical images." *LECTURE NOTES IN COMPUTER SCIENCE* **1205**, pp. 213–222, 1997.
7. T. Pock, R. Beichel & H. Bischof. "A novel robust tube detection filter for 3d centerline extraction." *Proc. 14th Scandinavian Conf. Image Analysis* pp. 481–490, 2005.
8. C. Kirbas & F. Quek. "Vessel extraction techniques and algorithms: a survey." *Bioinformatics and Bioengineering* Jan 2003.
9. S. Makita, T. Fabritius & Y. Yasuno. "Quantitative retinal-blood flow measurement with three-dimensional vessel geometry determination using ultrahigh-resolution doppler optical coherence angiography." *Optics Letters* **33(8)**, pp. 836–838, Apr 2008.
10. R. Neji, J.-F. Deux, G. Fleury et al. "A kernel-based approach to diffusion tensor and fiber clustering in the human skeletal muscle." *INRIA Research report* **6686**, 2008.
11. M. Unger, T. Pock & H. Bischof. "Continuous globally optimal image segmentation with local constraints." *Computer Vision Winter Workshop* 2008.